A Methodology to Develop Reduced-Order Models to Support the Operation and Maintenance of Offshore Wind Turbines

Zi Lin,[a,1] Debora Cevasco[a] and Maurizio Collu[a]

[a] *Department of Naval Architecture, Ocean and Marine Engineering, University of Strathclyde, G4 0LZ, Glasgow, UK*

Abstract

From an operation & maintenance (O&M) point of view, it is necessary to model the aero-hydro-servo-elastic (AHSE) dynamics of each wind turbine but, on the other side, wind farms generally include hundreds of wind turbines. Simply using and linking several advanced, single wind turbine models of dynamics to represent a wind farm can be computationally prohibitive. To this end, this paper developed a reduced-order model (ROM), able to capture the relevant dynamics of the system for a specific failure, having a lower computational cost and therefore more easily scalable up to a wind farm level. First, a nonlinear AHSE model is used to derive the time-domain response of the wind turbine degrees of freedom (DOFs). The failure mode, its relevant DOF, and the relevant operational conditions during which the failure is likely to occur are identified. A linearisation of the nonlinear aero-hydro-servo-elastic-drivetrain (AHSE-DT) model is then carried out. Subsequently, a number of linear ROMs are developed based on the linear full-order system but excluding high-frequency states using the modal truncation (MT) method. For the targeted DOF (rotor torque signal) and the load cases simulated, the results from the linear ROMs showed that the blade modes are important to capture not only the DOF of extreme values, but also the DOF of high-frequency responses (above 1.5 Hz). The results from nonlinear ROMs showed that the ROM eliminating all the tower modes (rigid tower) is acceptable to capture the DOF of low-frequency response (below 0.5 Hz), as it has almost the same spectral responses as the full-order nonlinear model.

Keywords: Linearisation; aero-hydro-servo-elastic; dynamic response; reduced-order model; offshore wind turbine

Nomenclature

[1] Corresponding author.
E-mail address: z.lin.100@strath.ac.uk (Z. Lin).

Abbreviations

AHSE	Aero-hydro-servo-elastic
AHSE-DT	Aero-hydro-servo-elastic-drivetrain
BEM	Blade Element Momentum
BT	Balanced Truncation
CAPEX	Capital Expenditure
DOF	Degree of Freedom
DT	Drivetrain
ETM	Extreme Turbulence Model
FEA	Finite Element Analysis
FFT	Fast Fourier Transform
FinEX	Financial Expenditure
GRC	Gearbox Reliability Collaborative
GWEC	Global Wind Energy Council
LTI	Linear Time-invariant
MSE	Mean Squared Error
MT	Modal Truncation
NREL	National Renewable Energy Laboratory
O&M	Operation & Maintenance
OP	Operating Point
OPEX	Operational Expenditure
PSD	Power Spectral Density
ROM	Reduced-order Model

SISO	Single Input, Single Output

Symbols

A	State Matrix
B	Input to Space Matrix
C	State to Output Matrix
D	Feedthrough Matrix
i	Member Index
n	Number of Values
P	Power Spectral Value
T	Input Torque
$\boldsymbol{u}$	System Input Vector
$\boldsymbol{x}$	State Vector
$\boldsymbol{y}$	System Output Vector

Subscripts

Λ_1, B_{x_1} and C_{x_1}	State-space matrices related to low-frequency states
Λ_2, B_{x_2} and C_{x_2}	State-space matrices related to high-frequency states
d_r	Pitch Circle Diameter
F_t	Transmitted Contact Force
$\boldsymbol{x_1}$	States with Low Frequencies
$\boldsymbol{x_2}$	States with High Frequencies

1. Introduction

Worldwide, wind power has grown rapidly since the 1990s. Based on the annually updated report from the Global Wind Energy Council (GWEC), the global installed wind power capacity has achieved over 539 GW, with successful commercial operations in over 90 countries [1]. Within the global wind power market (onshore and offshore), the offshore segment contributes 18.81 GW, representing the fastest-growing sector [1]. In the UK, offshore wind power is one of the essential components of the government's long-term strategy in carbon reduction. Being one of the most attractive locations for offshore wind investment, the UK has a power capacity of 8.7 GW in operation and 2.8 GW under construction [2].

Compared to onshore wind power, the offshore sector is less mature. One of the main obstacles for the offshore wind sector is the high cost of the investments for the assets, their installation, and their operation & maintenance (O&M), as the wind turbines and corresponding infrastructures have to survive in the harsher offshore conditions. The lifetime cost of wind farms can be related to two main components – Capital Expenditure (CAPEX) and Operational Expenditure (OPEX). Several studies identified potential approaches to reduce these expenditures. Dicotato et al. created a guideline of offshore wind economic development with the consideration of pre-investment and investment concerns [3]. Sarker and Faiz stated that the cost of offshore wind farms can be further minimised through an optimum selection in transportation and installation operations [4]. Feng and Shen assessed the design of non-uniform offshore wind farms through a capital cost model, to minimise the levelised cost of energy, testing the model on the base of the Horns Rev 1 offshore wind farm [5]. Ioannou et al. reported a lifecycle techno-economic framework of offshore wind turbines through a case study in the UK, which covered the components of CAPEX, OPEX and Financial Expenditure (FinEX) [6]. Most of the current researches analysing the cost-effectiveness of offshore wind turbine farms have mainly focused on the minimisation of the CAPEX. However, the O&M cost can represent up to 30% of the lifetime costs in an offshore wind farm [7], due to the high cost of inspecting and repairing and the harsh environment, which limits the safe-access to the structures. Only a few authors analysed in depth the OPEX aspect in their studies. Martin et al. conducted a sensitivity study regarding O&M cost in offshore wind farm operations [7]: the results concluded that the key factors increasing the OPEX are the repair costs along with failure rates, regardless of minor or major repairs. Tuyet and Chou suggested using optimal maintenance schedules to enhance the cost-effectiveness of offshore wind turbine farms [8]. Tautz-Weinert et al. performed a sensitivity analysis on the maintenance decision in a Spanish wind farm, where a wind blade replacement was required to avoid a disastrous failure [9].

Offshore wind turbines are complex systems operating in a multi-phase environment, under various field conditions and loads. To date, wind turbine models of dynamics have been mainly used as design tools. Virtually no studies addressed the problem by developing a holistic, wind-farm coupled model of dynamics. Only a few research studies, indeed, have focussed

on the O&M phases, analysing electrical and/or mechanical faults and their impact on the other components. Currently, wind farms models have focussed mainly on the aerodynamic aspects, while from an O&M point of view there is a need to model the aero-hydro-servo-elastic (AHSE) aspects of each wind turbine. However, due to the prohibitive computational costs, it is not possible to simply scale up state-of-the-art AHSE models to represent hundreds of wind turbines, therefore it is necessary to adopt approaches that can retain the necessary accuracy but reduce the computational cost. Reduced-order models (ROMs) are well established and widely applied in a variety of areas [10], including static reduction [11], dynamic reduction [12] and balanced methods [13], and others. The majority of the ROMs rely on a linearisation of the nonlinear system, and the accuracy of the linear system is limited to a small perturbation around the operating point (OP). On the other hand, Guyan's condensation method [11] focussed on the reduction of stiffness and mass matrix, which is a static method. Its advantage lies in not losing the structural complexity but results in a non-preserved eigenvalue-eigenvector problem, due to the coupling of mass and stiffness matrix. An improvement to Guyan's method is the IRS reduction [12]. This method introduces a correction to the mass matrix; however, it has not been widely used due to its main limitation: producing inaccurate results for some modes, and its high computation cost [12]. The dynamic reduction method explicitly approximates the mass matrix but has the same additional computation cost as the IRS method [12]. It also includes a modification of the original finite element analysis (FEA) codes, making it even more computationally expensive, especially for offshore wind turbines, where a high number of rigid/elastic bodies are included [12]. All the above ROMs focus on the reduction of the system's mass and stiffness matrix, derived from the linearisation of the system equations of motion. Also based on the linearisation method, the balanced truncation (BT) approach deals with the reduction of the state-space matrix. It transforms the state-space matrix into a 'balanced' form without losing the system's stability and passivity [14]. Based on different numerical methods, BT can be further divided into Lyapunov balancing, stochastic balancing, bounded real balancing, and others [15].

In recent years, a considerable research effort has been directed toward the so-called concept of "Digital Twins", focussing on a physical-based model of large engineering systems [16]. A Digital Twins approach based on ROM has the advantage, over traditional FEA tools, of computational efficiency, while providing a high-fidelity model of the full system [16]. Currently, ROMs of wind farms have been mainly employed in the field of control theory, and mainly by the researchers modelling the electric and electronic dynamics aspects of the wind turbine. For instance, Ghosh and Senroy [13] applied the BT method to reduce the dynamics model of a farm, obtaining a ROM that retains the dynamic relationships between the variation in wind speed and the power output variations, accurately over a wide range of frequencies. However, the wind turbine structural and mechanical dynamics are substantially simplified, as they are represented by only one degree of freedom (DOF), the drivetrain rotational speed. Such approaches, thus, have failed to include the impact of the stochastic nature of the wind speed and the

effects of structural dynamics on the drivetrain, generator and other electrical parts. On the other hands, due to the inherently complex nature of jacket structures, many types of research have focussed on developing ROMs for the jacket-type wind turbines [17]. However, these reductions are limited to the jacket structures only. This paper aims to develop ROMs based on a nonlinear, full-order AHSE model, for an offshore monopile wind turbine system. The aim is to derive a ROM able to represent the dynamics of the DOF signal driving the failure mode with an accuracy comparable with the nonlinear full-order method, but at a fraction of the computational cost.

The main contributions to the knowledge gap in this paper is summarised as follows:

1) To date, wind turbine models of dynamics have mainly supported the phases contributing to the CAPEX and only in few cases, the analysis tools have been applied to the understanding of the turbine actual operational conditions and to the detection of incipient failures of the system in the farm. The ROM developed in this paper has focussed on the O&M phase.
2) Wind turbine models of dynamics including all the AHSE aspects is highly desired from an O&M point of view. However, wind farms generally include hundreds of wind turbines. Simply using and linking several advanced, single wind turbine models of dynamics to represent a wind farm can be computationally prohibitive. To tackle this problem, this paper presents a methodology to develop offshore wind turbine ROMs, able to capture the dynamics of the system for a specific failure with a lower computational cost, and therefore more easily scalable up to a farm level.
3) Currently, ROMs of wind farms have been mainly employed in the field of control theory, and mainly by the researchers modelling the electric and electronic dynamics aspects of the wind turbine. The wind turbine mechanical part is simplified through the rotor rotational DOF only, while from an O&M point of view, modelling all the AHSE aspects is highly desired. The linear and nonlinear models developed in this paper were based on a linearisation of the AHSE model. The linearisation was validated against the nonlinear model. A comprehensive comparison between linear, nonlinear, reduced and non-reduced models are discussed and their accuracy and efficiency have been compared.

The remainder of this paper is organised as follows: section 2 introduces the methods applied in this paper, including the wind turbine model of dynamics, the linearisation and the modal truncation (MT) ROM approach. Section 3 introduces the reference wind turbine considered for the case studies, and the corresponding environmental condition linked to the failure. A comparative study on reduced and full-order methods, be it linear or nonlinear, is critically compared and discussed in section 4 and section 5, respectively. Finally, a series of conclusions based on the ROM investigations in this paper are listed in section 6.

2. Methodology

The final aim is to develop a ROM able to model the dynamics of the key DOF linked to the specific failure, with an accuracy similar to the one achieved by the equivalent nonlinear full-order model. **Fig. 1** shows a flow diagram of the present approach. A nonlinear (full-order) AHSE model, accounting for the simplified dynamics of the modular drivetrain (aero-hydro-servo-elastic-drivetrain (AHSE-DT)) is used as a basis for the linearisation and the derivation of the ROM (a). In parallel, the most critical failure mode is identified (b). The failure is then investigated to identify a specific load case and a specific target DOF (c). A linearisation technique is then applied to the nonlinear system, at the OP representative of the load case identified (d). The DOFs time signals obtained with the nonlinear, full-order model are post-processed, to derive and rank the peak frequencies of each DOF (e). Finally, the relative linear ROM is developed, based on the MT method (g). In addition to the linear ROM method, a nonlinear ROMs is also developed to verify the linear ROM (f), following a similar procedure, but without linearising the nonlinear wind turbine system. The results are then compared and discussed, quantifying the features of each ROM and non-reduced methods (h).

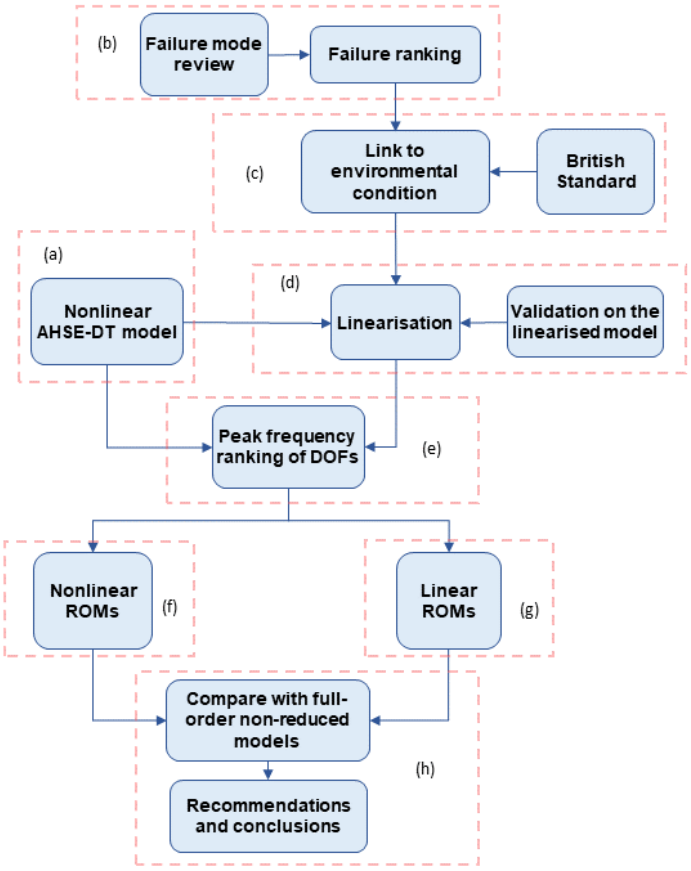

Figure 1 Process diagram of the methodology applied

2.1. Wind turbine model of dynamics

Fig. 2 shows the main features of the nonlinear AHSE-DT model used in this paper, based on FAST v8 [18], and in the following, a brief recap of the modelling approaches adopted is given. The aerodynamic forces on the single wind turbine are evaluated through the blade element momentum (BEM) theory, widely used in calculating aerodynamics of wind turbines. The BEM theory consists of two coupled sub-theories, the blade element theory and the momentum theory [19]. The main advantage of the BEM theory lies in transforming the 3D problem into a number of 2D problems, significantly reducing the numerical complexity, especially when compared with more advanced computational fluids methods. Further details on the BEM theory can be found in [19].

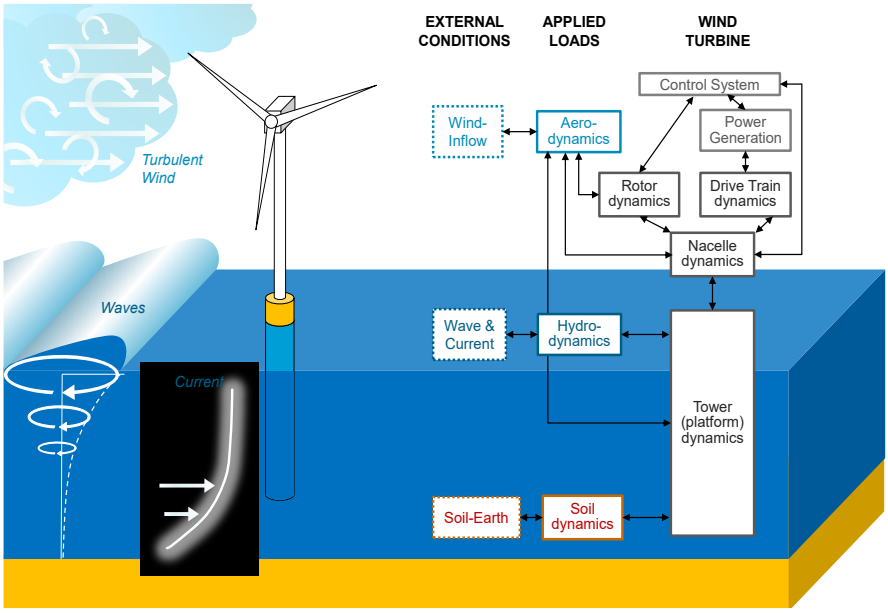

Figure 2: Modules in the AHSE-DT model. Adapted from [20]

Table 1 Definition of DOFs

DOFs - blades	DOFs - tower and others
Blade1 First edgewise mode	Drivetrain
Blade2 First edgewise mode	Generator Azimuth
Blade3 First edgewise mode	Nacelle Yaw
Blade1 First flapwise mode	First fore-aft tower bending mode
Blade2 First flapwise mode	First side-to-side tower bending mode
Blade3 First flapwise mode	Second fore-aft tower bending mode
Blade1 Second flapwise mode	Second side-to-side tower bending mode
Blade2 Second flapwise mode	
Blade3 Second flapwise mode	

The influence of the tower on the flow local to the blade is based on the downstream tower shadow model. The wind load on the tower and the tower shadow influence are calculated separately and superimposed. A combined multi-body and modal

analysis method is applied to determine the structural dynamic responses. The flexible elements, such as tower or blade, are modelled by a linear modal representation. For a three-bladed wind fixed offshore turbine, there are 16 DOFs in total for a full-order model (**Table 1**). For each blade, there is one edgewise model and two flapwise modes. Tower flexibility modes are realised through the fore-aft modes and the side-to-side bending modes, up to second order. The remaining three DOFs are the drivetrain rotational DOF, the generator azimuth and the nacelle yaw motion DOF.

Incident wave kinematics is modelled using Airy wave theory, for both regular and random waves. For regular waves, the wave elevation is modelled by a sinusoid wave with a certain frequency and amplitude. For random waves, superposition theory is applied, for which the irregular wave elevation is represented by a linear summation of different sinusoid waves. Wave forces are calculated using potential flow theory. Considering non-rotational, inviscid and incompressible problems, the wave-structural interaction problem can be determined by solving the Laplace equation, subject to a series of boundary conditions. The above-mentioned equations are solved numerically via the boundary element method in the frequency domain, considering different wave periods. Based on the Bernoulli's equation, wave diffraction forces are calculated in the frequency domain by an integral over the body surface using another solver, e.g. WAMIT [21]. Based on Cummins' [22] impulse response function theory, the first and second-order wave transfer functions are transferred from frequency domain to time domain using the Fourier Transform.

In order to maximise power generation and regulate generator speed, the baseline control was used for the National Renewable Energy Laboratory (NREL) 5 MW wind turbine [23] (collective blade-pitch control). Due to the method of linearisation applied in this paper, a simple variable-speed generator control is adopted for linear models. The generator has a rated speed of 1173.7 rpm and a rated torque of 43093.55 Nm. Further details on the baseline control for a 5MW reference wind turbine can be found in [23].

2.2. Linearisation

A wind turbine multi-body system is highly nonlinear. There are over a dozen DOFs, even for a single wind turbine. This paper applies the linearisation to build a linear time invariant (LTI), input-output equivalent system. Linearisation is realised by applying a state-space representation of the nonlinear system at the OP [20]:

$$\begin{cases} \dot{\mathbf{x}} = A\mathbf{x} + B\mathbf{u} \\ \mathbf{y} = C\mathbf{x} + D\mathbf{u} \end{cases} \tag{1}$$

The first step for linearisation is to determine an OP. Finding an OP is important for linearisation as the linear system is valid only from a small perturbation from an OP. In this paper, the OP is determined in the nonlinear time-marching process

through each sub-module. Further details on the linearisation for each sub-module and final matrix assembly can be found in [20].

2.3. Modal Truncation

The state-space equation in a vector form can be written as [24]:

$$\begin{cases} \begin{bmatrix} \dot{\mathbf{x}}_1 \\ \dot{\mathbf{x}}_2 \end{bmatrix} = \begin{bmatrix} \Lambda_1 & 0 \\ 0 & \Lambda_2 \end{bmatrix} \begin{bmatrix} \mathbf{x}_1 \\ \mathbf{x}_2 \end{bmatrix} + \begin{bmatrix} \mathrm{B}_{\mathbf{x}_1} \\ \mathrm{B}_{\mathbf{x}_2} \end{bmatrix} \mathbf{u} \\ \mathbf{y} = [\mathrm{C}_{\mathbf{x}_1} \quad \mathrm{C}_{\mathbf{x}_2}] \begin{bmatrix} \mathbf{x}_1 \\ \mathbf{x}_2 \end{bmatrix} + D\mathbf{u} \end{cases} \tag{2}$$

There are two types of MT approaches. In the first type, it is assumed that the transient phase of the response of the states characterised by high-frequency dynamics vanishes more quickly than the transient phases of the states characterised by a lower-frequency dynamics, while in the second type of MT it is assumed that the *derivatives* of the high-frequency states are the states to be truncated [25]. For a wind turbine system, it is difficult to justify at a physical level the truncation of only the derivative of a state. Therefore the first type of MT is here adopted. Under this condition, equation (2) becomes:

$$\begin{cases} \dot{\mathbf{x}}_1 = \Lambda_1 \mathbf{x}_1 + \mathrm{B}_{\mathbf{x}_1} \mathbf{u}, \dot{\mathbf{x}}_2 = \mathrm{B}_{\mathbf{x}_2} \mathbf{u} \\ \mathbf{y} = \mathrm{C}_{\mathbf{x}_1} \mathbf{x}_1 + D\mathbf{u} \end{cases} \tag{3}$$

3. Case Study

3.1. Wind turbine system definition

In this section, a case study based on the NREL 5 MW offshore wind turbine is introduced. Furthermore, a failure review is carried out to rank the severity of each failure mode. The most severe failure is then selected as the target for the ROM in this paper and the corresponding relevant environmental condition is identified.

Table 2 Properties of the 5MW wind turbine [23]

Parameters	Value
Rotor Orientation, Configuration	Upwind, 3 Blades
Control	Variable Speed, Collective Pitch
Drivetrain	High Speed, Multiple-Stage Gearbox
Rotor, Hub Diameter	126 m, 3 m
Hub Height	90 m
Cut-In, Rated, Cut-Out Speed	3 m/s, 11.4 m/s, 25 m/s
Cut-In, Rated Rotor Speed	6.9 rpm, 12.1 rpm
Rated Tip Speed	80 m/s
Rated Rotor Speed	12.1 rpm
Rated Generator Speed	1173.7 rpm
Gearbox Ratio	97 : 1
Electrical Generator Efficiency	94.4 %
Generator Inertia about High-Speed Shaft	534.116 kg•m^2
Equivalent Drive-Shaft Torsional-Spring Constant	867,637,000 N•m/rad
Equivalent Drive-Shaft Torsional-Damping Constant	6,215,000 N•m/(rad/s)

A fully coupled AHSE model based on the 5 MW reference wind turbine from the National Renewable Energy Laboratory (NREL) [18] is here adopted. The main characteristics of the wind turbine selected are shown in **Table 2**. For validation and comparison between ROMs and full-order methods, a list of system natural frequencies is shown in **Table 3**. The whole system's natural frequencies have a minimum value of around 0.3 Hz and the maximum natural frequency is the one of the tower's second-order bending modes, which is at around 3 Hz. The support structure adopted is a monopile [23], which is by far the most common foundation style [26]. In addition, a high-speed, geared drivetrain configuration has been considered.

Table 3 Full system natural frequencies [20]

Mode	Frequency (Hz)
1st Blade Asymmetric Flapwise Yaw	0.6664
1st Blade Asymmetric Flapwise Pitch	0.6675
1st Blade Collective Flap	0.6993
1st Blade Asymmetric Edgewise Pitch	1.0793
1st Blade Asymmetric Edgewise Yaw	1.0898
2nd Blade Asymmetric Flapwise Yaw	1.9337
2nd Blade Asymmetric Flapwise Pitch	1.9223
1st Tower Fore-Aft	0.3240
1st Tower Side-to-Side	0.3120
2nd Tower Fore-Aft	2.9003
2nd Tower Side-to-Side	2.9361
1st Drivetrain Torsion	0.6205

3.2. Critical failure mode and targeted DOF

This section explains and justifies the selection of the failure mode, its related DOF, around which the proposed ROMs are developed. Based on the data collected by Carroll et al. [27], Cevasco et al. (2018) [28] first identified and ranked the most critical components for a population of offshore wind turbines, representing the configuration most employed offshore and considered in this paper (geared system with an induction machine). Previous studies showed that the gearbox and DT have the longest downtime per failure [29]. Moreover, Wang et al. claimed that one of the major factors causing increased turbine downtime and reduced turbine reliability is the gearbox failure [30]. In agreement with that observed by [28], for the UK offshore round one structures, and tackled by the Gearbox Reliability Collaborative (GRC) project [31], the gearbox was shown to have the highest percentage of the total annual cost for unplanned maintenance operations. This is mainly due to the elevated average cost of the material for its repair, and the long repair time, for its relatively frequent major repairs and replacements.

The gearbox reliability and its failure inception identification have been two main areas of research for both onshore and offshore wind turbines. The GRC project concluded that *"most gearbox failures do not begin as gear failures or gear-tooth design deficiencies"*, but the failures *"...appear to initiate at several specific bearing locations under certain applications, which may later advance into the gear teeth as bearing debris and excess clearances cause surface wear and misalignments"*

[31]. By the combined use of full-scale dynamometer testing and high fidelity simulations, the top bearing and gears failure were identified and ranked per criticality [32].

The most severe failure selected and targeted in the present work is for the one related to the excessive tooth root bending stress deformation (for example, Salem et al. [33]), proportional to the transmitted contact force (F_t). The rationale behind this choice, over the possible failure of the rolling element of the bearing (roller and ring cracks [34] and wear [32]), is:

- the highest severity of the consequences of the failure. The gear wear and corrosion for contact stress, although more likely to happen [32], leads only to higher vibration and noise [35]. The high bending stress on the tooth from either high cycling fatigue or extreme loads, leads to tooth deformation and cracking, up to its final fracture.
- the identification of the possible environmental causes and related DOFs is more straight-forward for gears than bearings.

To support the latter observation, it must be noticed that, to identify the fundamental DOFs driving the failure, simplified modelling and physics considerations are preferred to more complex modelling. In general, higher complexity models (from multibody to finite element models) are used for the bearings dynamics and loads calculation [35]. On the other hand, Nejad et al. [36] showed that a simplified model can be sufficient to derive the main gear dynamics without the need for the multibody model. In these works, the simplified formulation for the transmitted contact force, expressed by assuming rigid bodies and contacts, zero damping gears, and neglecting their internal dynamics is:

$$F_t = \frac{2}{d_r} T \tag{4}$$

The input torque (T) to the gearbox is, thus, the DOF linked to the detection of the exceedance of the transmitted contact force, when considering the gear at the first stage of the gearbox (shown to be the one with higher criticality [36]).

3.3. Load cases definition

Once the relevant DOF for the detection of the gear root tooth bending failure has been identified, it is necessary to identify the environmental and operating conditions leading to the failure and its detection. As mentioned in section 3.2, the failure could be caused by either high cycling fatigue or loads in extreme operating conditions. On the latter, Nejad et al. [37] observed that wind speeds near cut-out hold the highest contributions in extreme loads on gears in normal operations. Dabrowski et al. [38] reached the same conclusion while conducting a study on the implementation of a storm controller for the reduction of the probability of gear tooth failure in the first planetary stage of the NREL 5 MW wind turbine. Independently from the type of controller, they observed that already at operating conditions, the transmitted force at the tooth has higher averaged values in the case of extreme turbulence model (ETM) employment. Dealing with a bottom-fixed structure, the influence of the wave

excitation on the drivetrain load can be neglected [38]. Additionally, Nejad et al. [39] showed that the load effect of the drivetrain components are mainly dependent on the axial force, the tower bending moment (a function of the thrust force), and the shaft torque (influenced by the power control system).

For these reasons, the wind-only load case for the wind turbine operating at 24 m/s under ETM has been set as reference load case for the following model order reduction simulations. The linearisation was carried at 24 m/s steady wind condition. **Fig. 3** shows a time history of the turbulent wind in x and y directions. The stochastic inflow turbulent wind was generated by TurbSim, a computer-aided pre-processing software by NREL [40]. The IEC Kaimal wind spectra model was applied to generate the inflow wind.

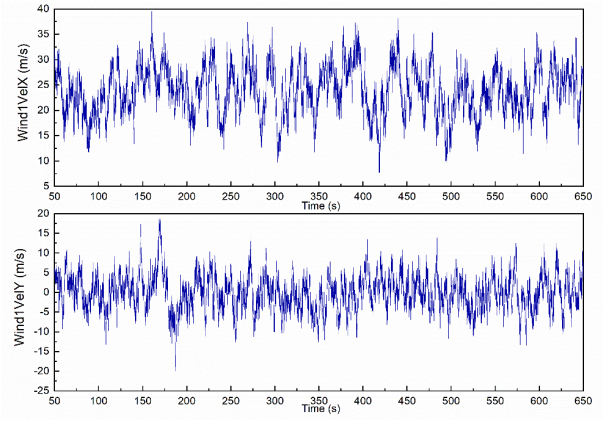

Figure 3 Wind speeds in X and Y direction

4. Linear ROMs

4.1. System linearisation method

The first step for linearisation is to determine an OP, which is a periodic steady-state condition of the system. At the OP, derivatives of the states are zero. It is important to set up the OP accurately as the linear representation of the nonlinear system is valid only for small perturbations around the OP. For setting up the OP, an initial rotor rotating speed equals 12.1 rpm has been selected. As the steady horizontal speed was 24m/s for ETM condition, we have focussed on the wind turbine operating in Region III [23]. Applying the baseline control [23], the corresponding blade pitch angle is 22.35 degree. After determining the OP, for the full-order model, a single input, single output (SISO) system with 32 states has been set up, for which the input was the wind speed and the output was rotor torque (**Fig. 4**). As the wind turbine blade was rotating during operation condition, the linearisations were carried out every 36-azimuth angles, in a total number of 10 realisations.

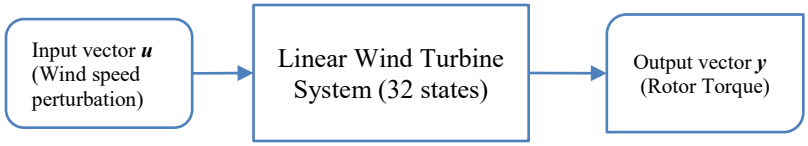

Figure 4 Linearized (full-order) system inputs and outputs

4.2. Validation of the nonlinear model

The linear models in the paper are based on the nonlinear AHSE model. Therefore, it is necessary to validate the nonlinear AHSE model against experimental data first. **Fig. 5** describes a comparison between the present results and experimental data. The 'present' results in **Fig.5** were carried at a series of steady wind conditions, ranging from cut-in to cut-out wind speeds, while the 'Repower-5MW' data is from the test of the Repower 5MW turbine [41]. As can be seen from the figure, there is a very good agreement between the present nonlinear AHSE model and experimental data.

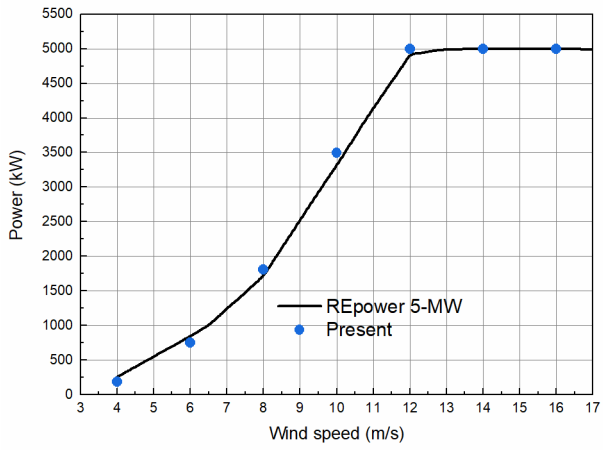

Figure 5 Validation of the nonlinear AHSE model

4.3. Validation of the linear model

For validation, a mono-direction step wind profile (**Fig. 6**) was chosen. The wind speed had an initial value of 24m/s and stepped up to 25m/s at 300s. The total simulation time is 650s. **Fig. 7 (a)** and **Fig. 8 (a)** are time histories of rotor torque and tower top fore-after deflection, respectively. The linear model at 24m/s showed a good agreement with the nonlinear results at 24 m/s steady wind condition. Since the linear results are confirmed around the OP only, there is a larger discrepancy between the nonlinear and linear results at 25m/s steady wind speed (**Fig. 7 (a)** and **Fig. 8 (a)**), compared with 24m/s steady wind condition. For the nonlinear models, spectra of rotor torque and tower fore-aft deflection are shown in **Fig. 7 (b)** and **Fig. 8**

(b). The spectrum was generated using the Fast Fourier Transform (FFT) method, with the inflow wind of 24m/s steady wind condition. As can be seen from the spectrum, the reason for the oscillation of the nonlinear model in tower top fore-aft deflection (**Fig. 8 (a)**) is due to the passenger of wind turbine blade in front of the tower, i.e. 3P, 6P, 9P and so forth, while the same phenomenon is problematic to be captured by the linear model. The oscillation magnitude of rotor torque in the nonlinear model of **Fig. 6 (a)** has seen a larger magnitude. The main reason for this is mainly due to the gearbox configuration of the drive train, compared with a direct drive configuration, which is consistent with a previous study [42].

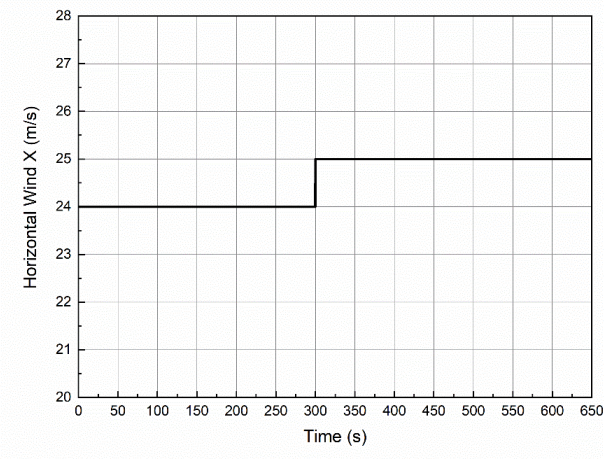

Figure 6 Step wind input profile

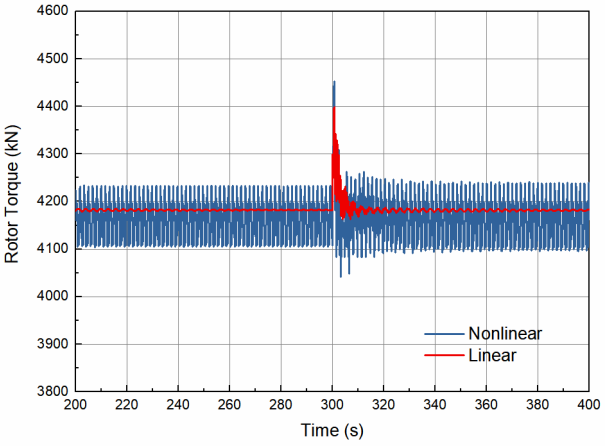

Figure 7 (a) Rotor torque, a comparison between full-order nonlinear and full-order linear model

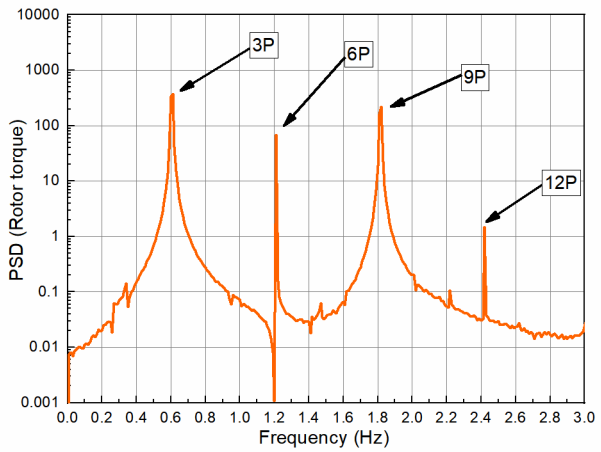

Figure 7 (b) Rotor torque spectrum, 24m/s steady wind condition

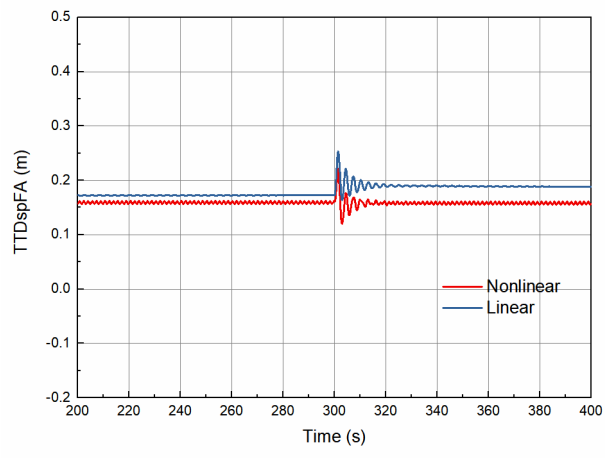

Figure 8 (a) Tower top fore-aft deflection, a comparison between full-order nonlinear and full-order linear model

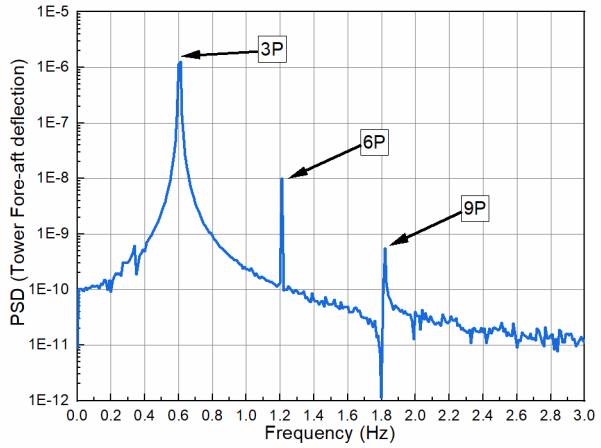

Figure 8 (b) Tower top fore-aft displacement spectrum (24m/s steady wind condition)

4.4. ROM based on the MT method

Fig. 9 shows the process of the MT ROM method applied in this paper. Under the ETM wind-only load condition chosen, based on the nonlinear AHSE-DT model outputs, the peak frequencies of each DOFs were identified through an FFT-spectral analysis. The definition of how the peak frequency was obtained on the tower's first side-to-side bending mode is shown in **Fig. 10**, which has a peak frequency of 0.34 Hz. The final ranking on the peak frequency results of each mode is shown in **Fig. 11**.

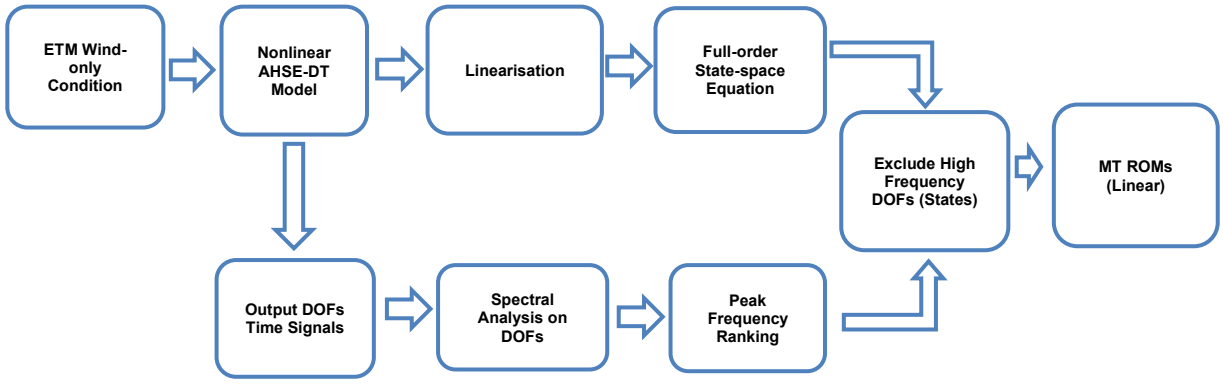

Figure 9 Process of MT ROM (linear)

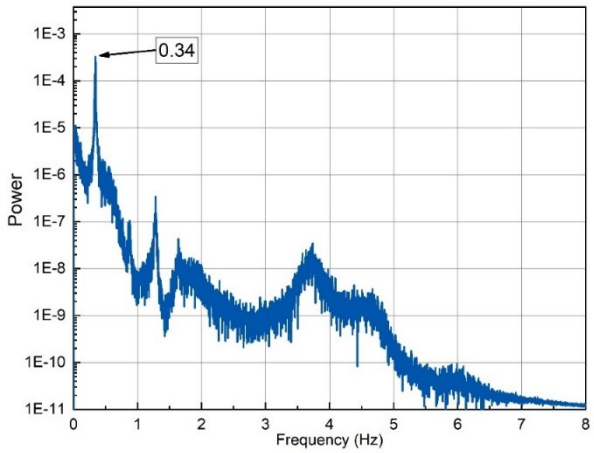

Figure 10 Definition on the peak frequency of each mode (example: tower's first side-to-side bending mode)

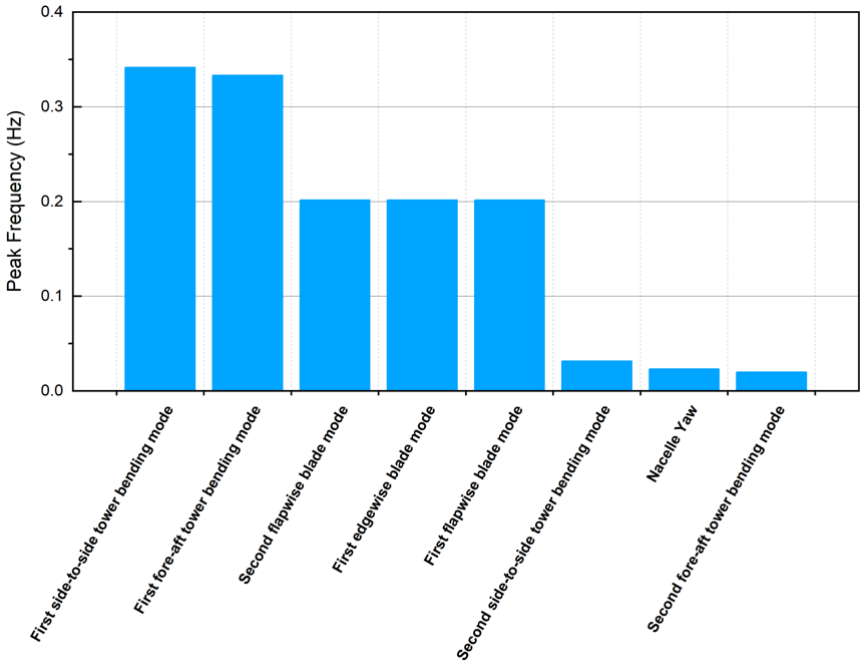

Figure 11: Ranking of peak frequencies for each DOF

Applying the linear SISO model with 32 states, two ROMs (MT1 and MT2) are developed by excluding high-frequency states. **Table 4** describes the corresponding DOFs enabled in MT1, MT2 and the full-order model. To comply with the aim of the model and the need to model a variable speed generator and a drive train with a gearbox, the DOFs linked to the generator and the drivetrain are always included. Apart from the drivetrain, yaw DOF and the generator, MT2 includes the tower's second-order bending mode only, while MT1 includes all of the DOFs in MT2 and three extra blade modes.

Table 4 List of case studies and DOFs considered-full-order linear and MT models

DOFs	Full-order Linear	MT1	MT2
First flapwise blade mode	✓	✓	
First edgewise blade mode	✓	✓	
Second flapwise blade mode	✓	✓	
Drivetrain	✓	✓	✓
Generator	✓	✓	✓
Yaw	✓	✓	✓
First fore-aft tower bending-mode	✓		
First side-to-side tower bending-mode	✓		
Second fore-aft tower bending-mode	✓	✓	✓
Second side-to-side tower bending-mode	✓	✓	✓

4.5. Comparisons between Linear ROM and Full-Order Nonlinear Model

In here, the results of the ROM of dynamics are evaluated and compared against the linear and nonlinear full-order methods. Due to the scholastic nature of the turbulent wind, each simulation included five realisations, and the simulation results were averaged across these five time signals. The initial 50s of the rotor torque time history is the transient part and

hence has not been considered. The rotor torque time predicted by the ROMs, including 14 DOFs (MT1) and 5 DOFs (MT2), are compared against that of the full-order methods (16 DOFs, full-order nonlinear and full-order linear), as summarised in **Table 4**. Due to the periodic steady linearisation process, it is difficult to include blade pitch control into the linearisation study. For comparison, nonlinear, full-order results were carried out under with and without blade pitch control conditions.

The torque signal mean values predicted by full-order linear and MT1 have an excellent agreement with the nonlinear full-order model (w/o pitch control) (**Fig. 12**, **Fig. 13** and **Table 5**). Excluding the pitch control results in a rotor torque mean value 10% larger (**Fig. 13** and **Table 5**). Compared with the nonlinear full-order model (w/o pitch control), extreme values (min and max) of MT1 have seen discrepancies but the difference is less than 10% (**Table 5**). Moreover, for linear models, removing the tower's first bending modes has no significant effects on rotor torque maximum values (comparisons between MT2 and full-order linear and nonlinear methods). In other words, in predicting rotor torque maximum values, the tower's first order bending mode is not strongly coupled with other modes.

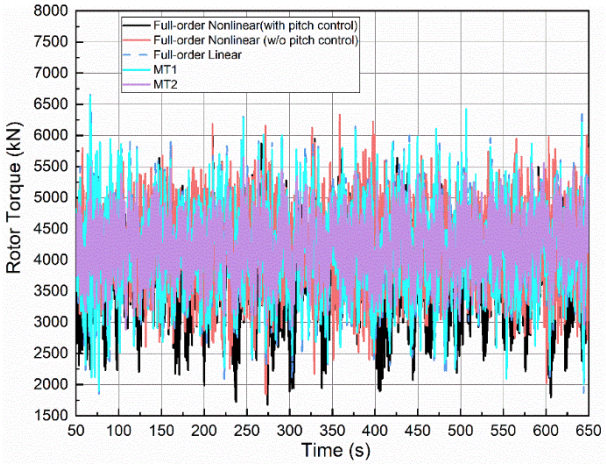

Figure 12 (a): Comparison of rotor torque time history-nonlinear full-order and linear methods (one realisation)

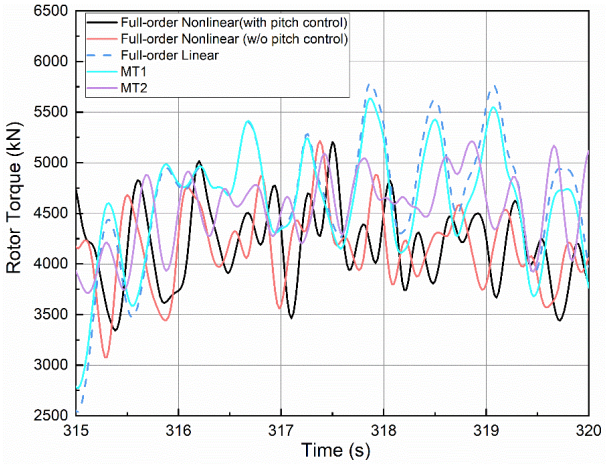

Figure 12(b): Comparison of rotor torque time history- nonlinear full-order and linear methods - close up (one realisation)

Table 5 Rotor torque time signal statistical characteristics - comparison of the different modelling approaches

	Full-order Nonlinear (with pitch control)	Full-order Nonlinear (w/o pitch control)	Full-order Linear	MT1	MT2
Min	1447.76	1922.60	1866.00	1928.39	2787.20
Max	6010.2	6140.00	6636.13	6554.89	5802.28
StD	671.52	529.95	650.44	621.77	407.73
Mean	3726.29	4181.41	4182.77	4183.03	4222.30

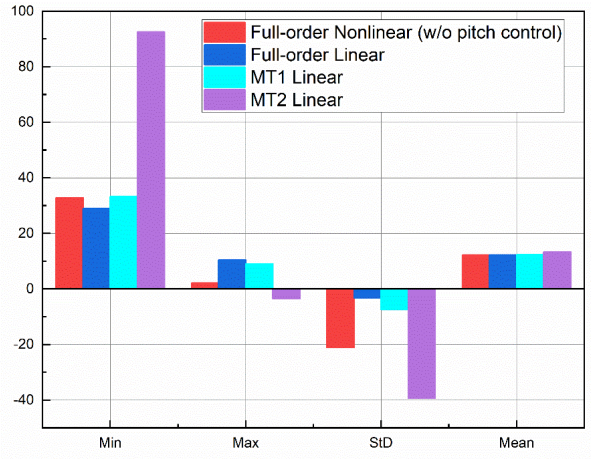

Figure 13: Comparison of statistical data, normalised against the full-order nonlinear method (with pitch control), time history

The spectrum of the torque signal obtained with MT1 shows a good agreement with the one of the full-order linear model, except for frequencies below 0.5Hz (**Fig. 14**), which is due to MT1 not taking into consideration the tower's first bending modes (both fore-aft and side-to-side). Although MT2 has a relatively good agreement with the nonlinear, full-order results, in terms of mean values (**Table 5** and **Fig. 13**), the results obtained by MT2, which excludes all of the blade modes, are apparently inaccurate, especially in terms of rotor torque spectrum above 0.5 Hz (**Fig. 14**). One possible reason for this inaccuracy and other discrepancies, may derive from the non-consistency of wind input between linear and nonlinear approaches. For nonlinear models, the turbulent inflow wind was evaluated in TurbSim under ETM condition with the IEC Kaimal spectrum. Although the wind direction, which is in consistent with the direction of the tower's fore-aft bending mode, remains unchanged, the turbulence will influence the responses on the blade motion and finally influence the corresponding rotor torque prediction. A further comparison of the spectra obtained with the different modelling approaches are listed in **Table 6**, quantified using the mean squared error (MSE), which is defined as follows:

$$MSE = \frac{1}{n}\sum_{i=1}^{n}\left[\frac{(P_{Full-order\ Nonlinear\ with\ pitch\ control})_i-(P_{models})_i}{(P_{Full-order\ Nonlinear\ with\ pitch\ control})_i}\right]^2 \quad (5)$$

$$models = \begin{cases} Full-order\ Nonlinear\ (w/o\ pitch\ control) \\ Full-order\ Linearised \\ Reduced\ Linearised \end{cases}$$

MSE of the full-order non-linear (w/o pitch control) indicates that it is the closest to the full-order nonlinear (with pitch control) method. The MSE gradually increased to 4.99 for MT2 linear, which shows the same trends as the spectrum (**Fig. 14**).

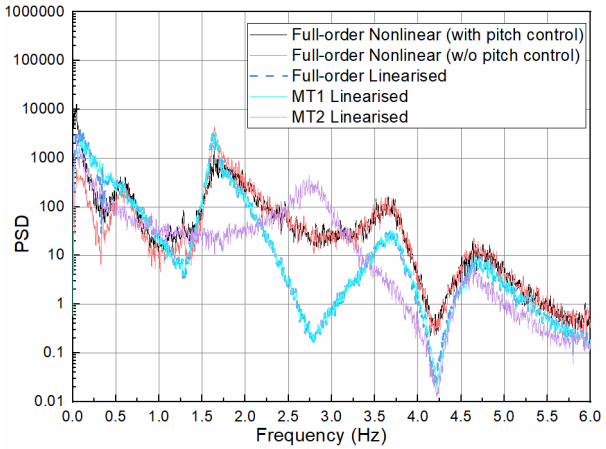

Figure 14: Comparison of rotor torque spectrum- nonlinear full-order and linear methods

Table 6 Comparison of MSE with nonlinear models (with pitch control)-spectrum

	Full-order Non-linear (w/o pitch control)	Full-order Linear	MT1 Linear	MT2 Linear
MSE	0.27251	1.28515	1.64143	4.99496

Apart from wind profiles, as discussed regarding the extreme values (**Table 5** and **Fig. 13**), another reason for the less accurate results given by MT2 may be due to the exclusion of the blade modes, i.e. under the ETM condition, the rotor torque response is dominated more by the blade modes than the tower modes. To verify it, an alternative ROM (MT3), excluding all the tower modes, is studied. Similar to the procedure described before, a comparison of the torque time signals and their spectra are shown in **Fig. 15**, **Fig. 16** and **Fig. 17**. As we can see, there is a marked improvement in extreme values (**Table 7** and **Fig. 17**). The differences between the torque spectra obtained with the MT3 and with the full-order linear model are relatively small, especially if compared with MT2. This phenomenon also showed that not only the coupling effects between DOFs, but also the linearisation process contribute to the differences between ROMs and full-order nonlinear models, as linearisation is only valid around a small perturbation of the OP. The high MSE of MT3 (**Table 8**) probably derives from the difference in the frequency range below 1.5 Hz, where the difference in the absolute value of power is much higher than that of the other frequency ranges, and hence has a much significant influence on MSE. So far, the main focus of this paper has been on linear

ROMs, while nonlinearities may have an effect on the dynamics of wind turbine structures, especially for low-frequency responses. The next session will investigate nonlinear ROMs.

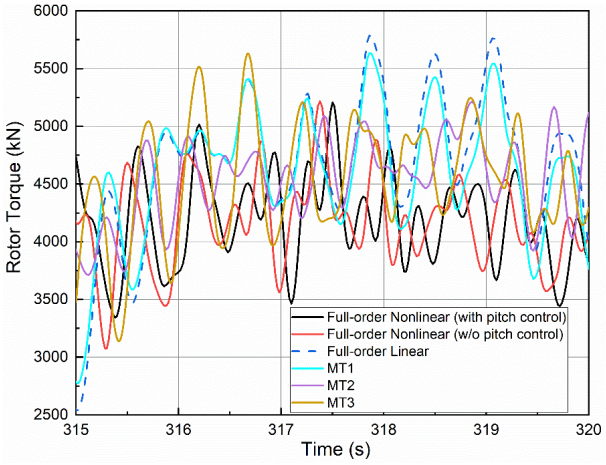

Figure 15 Comparison of rotor torque time history-nonlinear full-order and linear methods, MT3 added

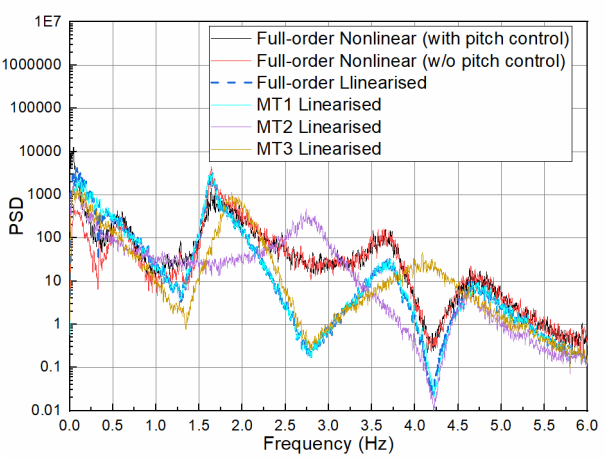

Figure 16 Comparison of rotor torque spectrum-nonlinear full-order and linear methods, MT3 added

Table 7 Statistical data of nonlinear full-order method and linear method – rotor torque time history (kN)

	Full-order Nonlinear (with pitch control)	MT3
Min	1447.76	2428.94
Max	6010.2	6033.15
StD	671.52	471.38
Mean	3726.29	4182.17

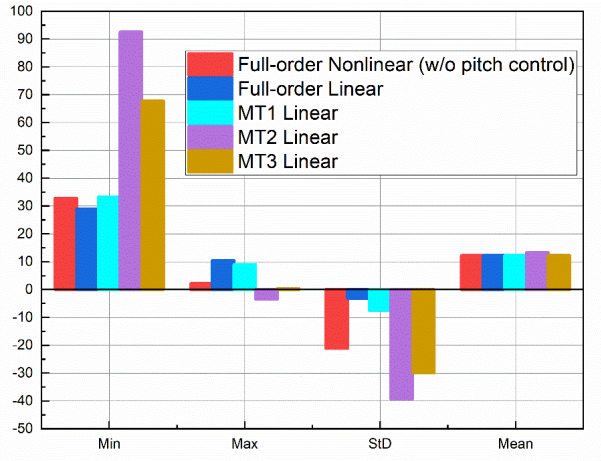

Figure 17 Comparison of statistical data, normalised against full-order method-time history, MT3 added

Table 8 Comparison of MSE with nonlinear models-spectrum

	Full-order Nonlinear (w/o pitch control)	MT3 Linear
MSE	0.27251	91.26412

5. Non-linear ROMs

5.1. Methodology

The advantage of MT ROM, as discussed previously, compared with other ROMs, is its capability of selecting which state to include/exclude in a state-space model. As we know, a state in the state-space equation corresponds to a DOF (or its time derivative) in the nonlinear motion equation. Since we have developed an approach to exclude high-frequency states (section 4.4), focussing on the nonlinear equation of motion, the corresponding DOFs to be excluded can be known. **Fig. 18** shows the process to derive the nonlinear ROMs adopted in this paper. Based on the full-order nonlinear AHSE-DT model, the time history of the rotor torque signals was generated. As was pointed out in section 3.3, an ETM wind-only condition was selected as environmental condition. Using the same peak frequency ranking in **Fig. 10**, two nonlinear ROMs are developed. The DOFs modelled in each ROM are the same as in **Table 4**, with the only difference being that now the ROMs are based on a nonlinear AHSE-DT model. In addition, a nonlinear ROM including the same DOFs as MT3 linear, as discussed in the previous session, is also developed and analysed. All the nonlinear ROMs and the corresponding full-order results were simulated, enabling the baseline pitch control.

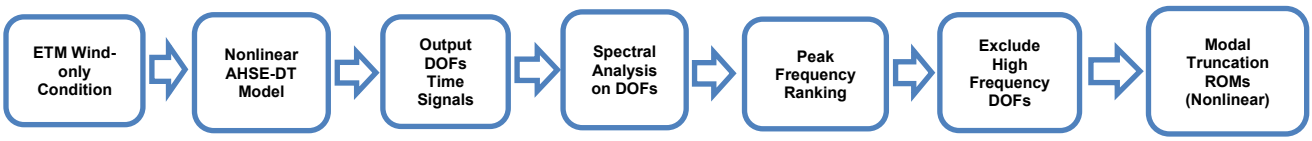

Figure 18 Process of nonlinear MT

5.2. Results and discussions

As we can see from **Fig. 19**, the mean rotor torque resulting from all the nonlinear ROMs are in a remarkable agreement with the full-order nonlinear models, which is the same as the linear ROMs. The rotor torque time signal, obtained with the nonlinear MT2, is more variable than for the other ROMs (**Table 9**), or for the full-order nonlinear models. In addition, a better agreement on extreme values (**Table 9** and **Fig. 20**) can be observed for the MT2 nonlinear, compared with the MT2 linear. The StD of rotor torque predicted by MT3 is within 10% difference, showing a better agreement compared to the MT1 nonlinear, which has two extra modes.

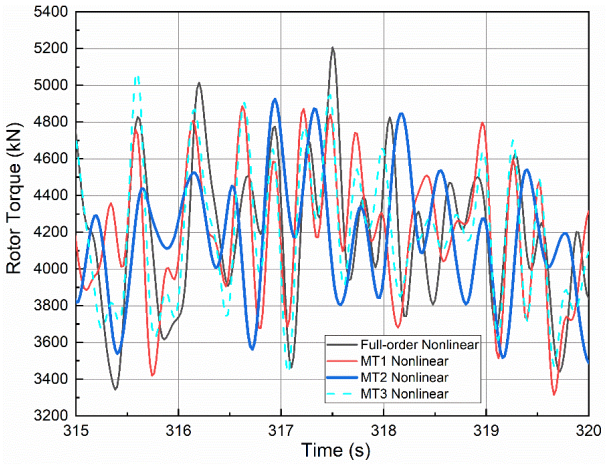

Figure 19 Comparison of rotor torque time history- nonlinear full-order and nonlinear ROMs - close up

Table 9 Statistical data of nonlinear full order method and nonlinear ROMs – rotor torque time history (kN)

	Full-order Nonlinear	MT1 Nonlinear	MT2 Nonlinear	MT3 Nonlinear
Min	1447.76	1280.66	2040.00	1313.36
Max	6010.2	6352.60	5503.80	6426.20
StD	671.52	722.40	594.44	700.49
Mean	3726.29	3726.34	3734.59	3727.57

In the previous section, we have discussed the potential reasons for the large discrepancies in MT2 being the blade modes and nonlinearities. From **Fig. 20**, there is a marked improvement for MT2 when applying the nonlinear model: it shows a decent agreement compared with the full-order nonlinear model for frequency range below 0.5 Hz (**Fig. 21**). Compared with MT1 nonlinear and MT2 nonlinear, the MT3 nonlinear is characterised by a better agreement with the full-order, non-linear model, in the frequency range between 0.5Hz and 1.0Hz. As we can see from **Table 10**, the MSE of MT1 is much higher than MT2, which has a similar reason when it comes to MT3 linear. The peaks of MT1 in the frequency range between 0.5 and 1.5 Hz (**Fig.21**) have a much greater contribution from the absolute value of the power. MT3 has seen a discrepancy in the frequency

range above 3Hz (**Fig.21**) but having some smaller contributions to the MSE due to the much smaller value of the power spectra at frequency range above 3.0 Hz.

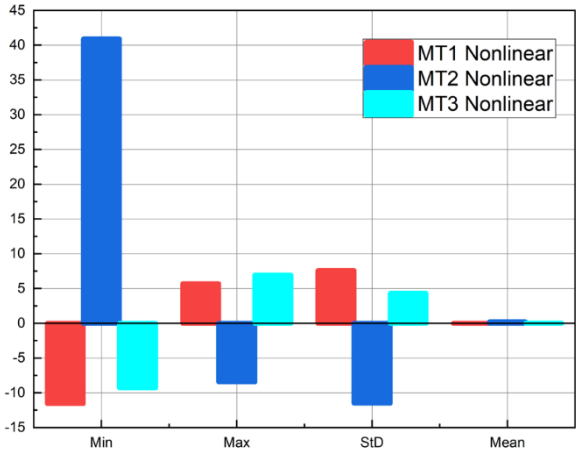

Figure 20 Comparison statistical data, normalised against full-order method-time history

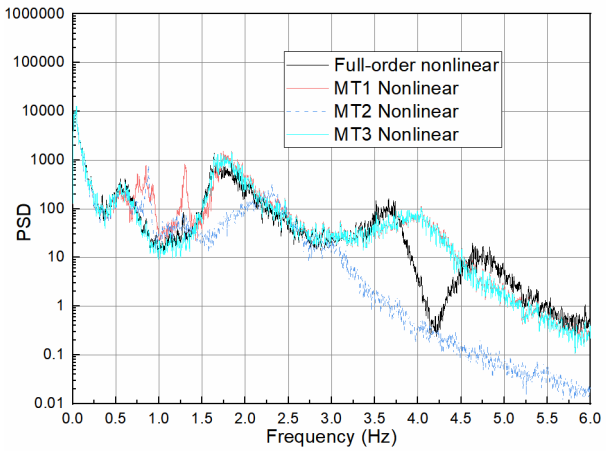

Figure 21 Comparison of rotor torque spectrum - nonlinear full-order and nonlinear ROMs

Table 10 Comparison of MSE against nonlinear full-order models–spectrum

	MT1 nonlinear	MT2 Nonlinear	MT3 Nonlinear
MSE	217.27352	2.02587	188.98563

In the following section, a comparison between the computational costs of the different models is given. As discussed in the introduction, a single wind turbine includes more than a dozen DOFs, and a wind farm usually consists of hundreds of wind turbines. Simply scaling up the AHSE-DT model for each wind turbine to represent a wind farm could be very time-consuming. The advantage of the ROMs in terms of simulation time is shown in **Fig. 22**. Without considering the time taken by the linearisation process, i.e. to generate the state-space matrix (which has to be done only once), the simulation time consumed of linear models is only around 7% of the nonlinear, full-order model, while nonlinear ROMs take almost the same time as the full-order nonlinear method. The processing time of the nonlinear full-order model, on a Windows PC (Intel ® Core i7-3770

CPU @ 3.40GHz, 8GB RAM) is 8.06 minutes for a 10.83-min real-time simulation. The processing time for the reduced MT3 nonlinear model is around 0.32 min shorter than the full-order, non-linear model. Although this may not seem a substantial reduction in time, it has to be considered that this is relative to a single wind turbine, and a single load case. The vision of the paper is to develop techniques suitable for the AHSE coupled model of dynamics simulations of whole wind farms, and over several load cases. For example, considering current and future offshore wind farms in the UK, around 150-200 wind turbines can be present in a farm, and the number of load cases considered can be of the order of thousands: the small temporal advantage for one single wind turbine and one load case then translates into months of saved computational time for a farm over several load cases.

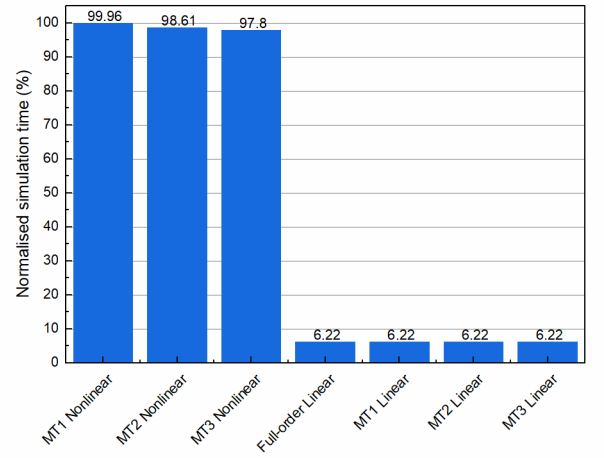

Figure 22 Total simulation time, normalised against the full-order nonlinear method (%)

6. Conclusions

This paper has developed a series of ROMs, for a single offshore wind turbine, aimed at capturing the dynamics of a key DOF, linked to a specific failure, with an accuracy similar to the full-order, non-linear model, but with a reduced computational cost. Both linear and nonlinear ROMs were developed, and their results were compared with the nonlinear full-order model to explain the inherent coupling effects and correctness of each proposed ROM. Based on the case study results, the following conclusions have been reached:

- Linear models are recommended for evaluating the mean value only. Extreme values are not well predicted by the linear results.

- Rotor torque is more sensitive to blade modes than tower modes. ROMs including all the blade modes while excluding all the tower modes have better results compared with ROMs with only a select number of tower and blade modes.
- Spectral analysis demonstrates that the non-linear effects have an essential contribution to the rotor torque signal in the frequency range below 0.5Hz. If the failure falls into the frequency range below 0.5Hz, nonlinear models should be applied, as the linear models failed to accurately capture the characteristics of the torque signal, compared with the full-order model.
- For reduced models, the adoption of nonlinear methods resulted in a slight reduction of computational time that for a single wind turbine and a single simulation may not be significant, but when considering a typical wind farm (150 ~ 200 turbines) and the number of simulations to cover the load cases (10^3 order), the simulation time saved can be in the order of months.
- Linear ROMs provide an easier and faster way to study the coupling effects between DOFs, as it can save up to 93% of the simulation time compared with nonlinear, full-order models.

Acknowledgements

The work presented is supported by the UK Engineering and Physical Sciences Research Council (EPSRC) HOME-Offshore project (EPSRC Reference: EP/P009743/1). The second author is supported by grant EP/L016303/1 for the University of Strathclyde, Cranfield University and the University of Oxford, Centre for Doctoral Training in Renewable Energy Marine Structures - REMS (http://www.rems-cdt.ac.uk/) from the UK Engineering and Physical Sciences Research Council (EPSRC).

References

[1] Global Wind Energy Council (GWEC). Global Wind Energy Report: Annual Market Update 2017. 2018.

[2] Smith M, Backwell B, Medic N. Offshore Wind Energy - Powering the UK since 2000 2019. https://events.renewableuk.com/images/Images/2019/GOW19/HAYNES-OFFSHORE-WEBSITE-VERSION.pdf.

[3] Dicorato M, Forte G, Pisani M, Trovato M. Guidelines for assessment of investment cost for offshore wind generation. Renew Energy 2011;36:2043–51. doi:10.1016/j.renene.2011.01.003.

[4] Sarker BR, Faiz TI. Minimizing transportation and installation costs for turbines in offshore wind farms. Renew Energy 2017;101:667–79. doi:10.1016/j.renene.2016.09.014.

[5] Feng J, Shen WZ. Design optimization of offshore wind farms with multiple types of wind turbines. Appl Energy 2017;205:1283–97. doi:10.1016/j.apenergy.2017.08.107.

[6] Ioannou A, Angus A, Brennan F. A lifecycle techno-economic model of offshore wind energy for different entry and exit instances. Appl Energy 2018;221:406–24. doi:10.1016/j.apenergy.2018.03.143.

[7] Martin R, Lazakis I, Barbouchi S, Johanning L. Sensitivity analysis of offshore wind farm operation and maintenance cost and availability. Renew Energy 2016;85:1226–36. doi:10.1016/j.renene.2015.07.078.

[8] Nguyen TAT, Chou SY. Maintenance strategy selection for improving cost-effectiveness of offshore wind systems. Energy Convers Manag 2018;157:86–95. doi:10.1016/j.enconman.2017.11.090.

[9] Tautz-Weinert J, Yürüşen NY, Melero JJ, Watson SJ. Sensitivity study of a wind farm maintenance decision - A performance and revenue analysis. Renew Energy 2019;132:93–105. doi:10.1016/j.renene.2018.07.110.

[10] Rezaei MM, Behzad M, Haddadpour H, Moradi H. Development of a reduced order model for nonlinear analysis of the wind turbine blade dynamics. Renew Energy 2015;76:264–82. doi:10.1016/j.renene.2014.11.021.

[11] Guyan RJ. Reduction of stiffness and mass matrices. AIAA J 1965;3:380–380. doi:10.2514/3.2874.

[12] Flanigan CC. Model reduction using Guyan, IRS, and Dynamic methods. Proc Int Modal Anal Conf IMAC 1998;1:172–6.

[13] Ghosh S, Senroy N. Balanced truncation based reduced order modeling of wind farm. Int J Electr Power Energy Syst 2013;53:649–55. doi:10.1016/j.ijepes.2013.05.032.

[14] Gugercin S, Antoulas AC. A survey of model reduction by balanced truncation and some new results. Int J Control 2004;77:748–66. doi:10.1080/00207170410001713448.

[15] Antoulas AC. A survey of model reduction methods for large-scale systems. Am Math Soc 2006;280:1–28. doi:10.1080/00207170410001713448.

[16] Knezevic D. Enabling High-Fidelity Digital Twins of Critical Assets Via Reduced Order Modeling n.d.

[17] Song H, Damiani R, Robertson A, Jonkman J. A new structural-dynamics module for offshore multimember substructures within the wind turbine computer-aided engineering tool FAST. Proc 23rd Int Offshore Polar Eng Conf 2013;9:383–91.

[18] Jonkman BJ, Jonkman JM. FAST v8.16.00a-bjj User's Guide 2016:58.

[19] Moriarty PJ, Hansen AC. AeroDyn Theory Manual. vol. 15. 2005. doi:10.1146/annurev.fl.15.010183.001255.

[20] Jonkman JM, Jonkman BJ. FAST modularization framework for wind turbine simulation: Full-system linearization. J Phys Conf Ser 2016;753. doi:10.1088/1742-6596/753/8/082010.

[21] WAMIT® WAMIT, Inc. n.d. http://www.wamit.com/.

[22] Cummins WE. The impulse response function and ship motions. Symp. Sh. Theory, Institut Flir Schiffbau Der

Universitit Hamburg: 1962.

[23] Jonkman J, Butterfield S, Musial W, Scott G. Definition of a 5-MW Reference Wind Turbine for Offshore System Development 2009. doi:10.2172/947422.

[24] Chen C-T. Linear System Theory and Design. Third. Oxford University Press; 1999.

[25] Lee Y, Seo B, Lee E-T. Application of model reduction techniques to jacket structures. Int J Steel Struct 2015;15:1–6. doi:10.1007/s13296-014-1101-6.

[26] Gentils T, Wang L, Kolios A. Integrated structural optimisation of offshore wind turbine support structures based on finite element analysis and genetic algorithm. Appl Energy 2017;199:187–204. doi:10.1016/j.apenergy.2017.05.009.

[27] Carroll J, McDonald A, McMillan D. Failure rate, repair time and unscheduled O&M cost analysis of offshore wind turbines. Wind Energy 2016;19:1107–1119. doi:10.1002/we.1887.

[28] Cevasco D, Collu M, Lin Z. O&M Cost-Based FMECA: Identification and Ranking of the Most Critical Components for 2-4 MW Geared Offshore Wind Turbines. J Phys Conf Ser 2018;1102. doi:10.1088/1742-6596/1102/1/012039.

[29] Artigao E, Martín-Martínez S, Honrubia-Escribano A, Gómez-Lázaro E. Wind turbine reliability: A comprehensive review towards effective condition monitoring development. Appl Energy 2018;228:1569–83. doi:10.1016/j.apenergy.2018.07.037.

[30] Wang F, Chen J, Xu B, Stelson KA. Improving the reliability and energy production of large wind turbine with a digital hydrostatic drivetrain. Appl Energy 2019;251:113309. doi:10.1016/j.apenergy.2019.113309.

[31] Musial W, Butterfield S, McNiff B. Improving Wind Turbine Gearbox Reliability. Eur. Wind Energy Conf. 2007, Milan, Italy: 2007, p. 1–13. doi:10.1007/978-3-319-09918-7_20.

[32] Link H, Lacava W, Dam J Van, Mcniff B, Sheng S, Wallen R, et al. Gearbox Reliability Collaborative Project Report : Findings from Phase 1 and Phase 2 Testing 2011:85. doi:10.2172/1018489.

[33] Salem A, Abu-Siada A, Islam S. Application of Order Analysis to Diagnose Fatigue within Wind Turbine Gearbox. Technol Econ Smart Grids Sustain Energy 2017:3–7. doi:10.1007/s40866-016-000017-y.

[34] Herr D, Heidenreich D. Understanding the Root Causes fo Axial Cracking in Wind Turbine Gearbox Bearings. Issue 03 2015:38–45.

[35] Nejad AR, Gao Z, Moan T. Fatigue reliability-based inspection and maintenance planning of gearbox components in wind turbine drivetrains. Energy Procedia 2014;53:248–57. doi:10.1016/j.egypro.2014.07.234.

[36] Nejad AR, Gao Z, Moan T. On long-term fatigue damage and reliability analysis of gears under wind loads in offshore wind turbine drivetrains. Int J Fatigue 2014;61:116–28. doi:10.1016/j.ijfatigue.2013.11.023.

[37] Nejad AR, Gao Z, Moan T. Long-term analysis of gear loads in fixed offshore wind turbines considering ultimate operational loadings. Energy Procedia 2013;35:187–97. doi:10.1016/j.egypro.2013.07.172.

[38] Dabrowski D, Natarajan A. Assessment of gearbox operational loads and reliability under high mean wind speeds. Energy Procedia 2015;80:38–46. doi:10.1016/j.egypro.2015.11.404.

[39] Nejad AR, Bachynski EE, Li L, Moan T. Correlation between Acceleration and Drivetrain Load Effects for Monopile Offshore Wind Turbines. Energy Procedia 2016;94:487–96. doi:10.1016/j.egypro.2016.09.219.

[40] NWTC Information Portal (TurbSim). https://nwtc.nrel.gov/TurbSim. Last modified 14-June-2016 ; Accessed 18-December-2018 n.d.

[41] Ochs DS, Member GS, Miller RD, Member S, White WN. Simulation of Electromechanical Interactions of Permanent-Magnet Direct-Drive Wind Turbines Using the FAST Aeroelastic Simulator. IEEE Trans Sustain Energy 2014;5:2–9. doi:10.1109/TSTE.2013.2269681.

[42] Slot RMM, Svenningsen L. Consistent direct-drive version of the NREL 5MW turbine. WindEurope, 2018.